THE AMERICAN SOCIETY OF MECHANICAL ENGINEERS
345 E. 47th St., New York, N.Y. 10017

96-TA-13

REDUCTION OF TIP CLEARANCE LOSSES THROUGH 3-D AIRFOIL DESIGNS

J. Brent Staubach
Om P. Sharma
Gary M. Stetson
Pratt and Whitney
E. Hartford, CT. 06108

ABSTRACT

Results are presented from a program, conducted to investigate the impact of spanwise stacking of turbine airfoil sections on tip clearance flows. Numerical as well as physical experiments were performed to demonstrate that these airfoils yielded about 40% reduction in tip clearance losses compared to those designed with a conventional approach. Three dimensional, steady Euler and Reynolds Averaged Navier Stokes (RANS) codes were used to execute the numerical experiments. Initial physical experiments were performed in a water tunnel by using linear cascades to validate the design concepts. The verification of the overall design concepts was executed in an uncooled full scale rotating rig

BACKGROUND

Improvements in reliability, durability, fuel consumption, purchase price, and maintenance cost are required to meet current and future market demands. In gas turbines these demands will result in smaller diameters, higher mechanical speeds, fewer stages, fewer airfoils per stage, and reduced complexity of gas sealing techniques. As the size of the turbine reduces, the performance becomes more sensitive to physical clearance between stationary and rotating hardware, in particular the clearance between the rotor blade tip and the outer case. To maintain basic turbine parameters (flow coefficient and work coefficient), smaller turbines will operate at higher rotational speed. This higher speed will create mechanical/structural limitations in applying tip shrouds to minimize the impact of tip clearance on performance. There is, therefore, a need to develop technology which will allow the ability to achieve low levels of clearances between the rotor and the case or to create an aerodynamic design that reduces the performance deficit associated with tip clearance.

Minimizing physical tip clearance is difficult, but it can be achieved to within acceptable tolerances at a given operating condition. The real challenge is to control tip clearance at all operating conditions, especially through large transients. In the case of an aircraft engine, the speed and temperature levels can increase by a factor of two, within seconds, creating mechanical and thermal distortions. These distortions can cause the tip of the rotor airfoils to rub into the outer case, creating larger clearances than intended for all "steady" operating conditions. Although methods are available to minimize this effect, these are costly to develop and implement into an engine. The ideal situation is to design an outer case / rotor system with large enough clearance so rubs never occur during transient operations and provide the same performance as obtained at tight tip clearances. The intent of this work is to demonstrate that performance associated with the change of tip clearance can be influenced with the rotor airfoil aerodynamic design.

INTRODUCTION

The impact of tip clearance on turbine performance has been well documented through experimental programs conducted over the last fifty years. For unshrouded turbines operating under typical gaps between airfoils and the casing, tip leakage flows contribute between 0.5% to 4% loss in efficiency. Experimental and analytical research programs have been conducted over the last forty years to develop improved understanding of loss generation mechanisms induced by tip clearance flows. Basic experimental investigations (Ref. 1-6) have mostly focused on acquiring detailed information on tip leakage flows in a controlled environment (linear cascades). Results from these investigations indicate that real flow in tip regions is highly complex, consisting of separation bubbles on the tips and well defined vortical structures formed by the leakage of flow from the pressure to the suction side of the airfoil as indicated in Figure 1 (Ref. 2,3). These experiments have clearly shown that a portion of the tip leakage losses is due to viscous flow mechanisms in the airfoil tip region while mixing of the misdirected flow is responsible for the remainder of the losses. Although these investigations have highlighted the physics of

Presented at the 1996 ASME Turbo Asia Conference
November 5–7, 1996 — Jakarta, Indonesia

loss generation mechanisms, they have not provided clear guidelines to minimize the losses induced by tip flows.

Analytical investigations have concentrated on developing models for the formation and evolution of tip leakage vortex structures. Lifting line analyses (Ref. 7, 8) have been used to compute the secondary velocity flowfield as well as loss in efficiency stemming from the induced drag of the trailing vortex system. This approach requires empirical correlations for the tip vortex circulation and the vortex core size to arrive at realistic estimates of losses. Unavailability of universally applicable correlations have limited the usefulness of this approacb.

An alternative approach in this category has recently been developed for compressors (Ref. 9). The clearance velocity field in this approach is assumed to be divided into independent through flow (mainstream) and the cross flow (induced by the clearance vortex). This assumption permits the description of the tip leakage flow in terms of a two-dimensional unsteady flow imposed on the overall three-dimensional flow in the passage. This method has yielded accurate predictions of the tip leakage vortex trajectories inside and downstream of the rotor passage. This approach , however, has not been extended to predict losses generated by the tip leakage flows.

In spite of the complexity of the tip leakage flows, the change in efficiency due to change in clearance levels can be estimated within ± 1 % by using a fairly simple correlation. Experimental data are plotted in Figure 2 (Ref. 10) which shows that the change in efficiency is linearly related to the change in clearance as given :

$$\Delta\eta/\eta = k\,(\Delta Cl/h) \qquad [1]$$

where;
k is a constant of proportionality
η is efficiency
Δ**Cl** is change in clearance
h is the rotor airfoil height

Experimental data from additional turbine tests (Ref. 1) indicate that **"k"** in equation (1) is a function of tip reaction (static enthalpy drop in the rotor divided by the static enthalpy drop in the stage) as shown in Figure 3. This figure shows that a reduction in tip reaction is needed to counteract the effect of tip leakage loss. A reduction in reaction, however, results in increased rotor losses due to unfavorable pressure gradients in the airfoil and endwall regions. There is, therefore, a need to develop design approaches which will control flow in tip regions of rotors without adversely affecting the rotor performance.

A new insight into rotor airfoil tip flows was provided by experimental programs conducted at Pratt & Whitney in uncooled single and two stage turbines during the early 1980's. The main objectives of these programs was to minimize secondary losses in turbine stators through the use of a three-dimensional airfoil design approach. Experimental data were acquired for turbine stages having the same rotor but different upstream stators. Spanwise distributions of efficiency for the rotor operating at design with two different upstream stators are shown in Figure 4. Three sets of data are plotted in this figure. Two sets of data represent those acquired for the rotor with a conventional radial upstream stator with two different rotor tip clearances (1.0 and 1.5 x nominal clearance levels). The third set of data represents that acquired at nominal clearance for the rotor with "bowed" upstream stator. An expected change in efficiency in the outer 17% region is shown in this figure for the two levels of rotor clearance with conventional upstream stator. The efficiency profile with the "bowed" upstream stator, for rotor with nominal clearance, shows the same levels in the outer 20% region as those obtained with the 1.5x clearance operating with the radial (conventional) stator. This result indicates that the rotor with "bowed" upstream stator behaves as if it has 50% larger clearance. The bowed stator used in this test was designed to reduce flow in the endwall region for the stator passage and to increase it in the hub and the tip region for the rotor passage. This increased available flow in the tip region causes higher leakage and lower efficiency than the configuration with the base stator. Results from this experiment can be expressed in terms of equation (1) provided an additional factor is applied for the "3D" bowed stator (k_{3D}). Equation 1 is modified as shown below:

$$\Delta\eta/\eta = k k_{3D}\,(\Delta Cl/h) \qquad [2]$$

Where;
k_{3D} = **1.5** (for the bowed stator)

Based on the results shown in figures 2 and 3, the correlation given in equation 1 was reinterpreted as:

$$\Delta\eta \propto \textbf{(Tip Flow) / (Rotor Passage Flow)} \qquad [3]$$

This expression indicates that reducing flow in the tip region of turbine rotors has the potential to reduce performance loss due to tip clearance flows. A reduction in flow in tip regions can also be interpreted as reduction of "k_{3D}" in equation (2).

It is clear from the above discussion that tip clearance losses in turbine rotors can be regulated by controlling the flow in the tip regions This can be achieved through the design of the upstream stator. This paper extends this concept to the rotor airfoil designs to redistribute flow in the regions such that the performance sensitivity to clearance changes is substantially reduced.

This investigation was conducted in three phases. In the first phase, the predictive capability of a 3D Computational Fluid Dynamics (CFD) code was verified against experimental data obtained for an airfoil with tip clearance flows. Work in the second phase was directed toward developing design concepts which allow control of rotor tip clearance losses and the size of the tip leakage vortices. In this phase numerical and physical experiments were conducted in linear cascades. These experiments were utilized to generate guidelines on the impact of airfoil stacking changes on the size of the tip clearance vortices and their effect on performance. The verification of the design concepts was demonstrated in the third phase of the program. In this phase, rotor airfoil sections were stacked to minimize flow in the tip clearance region. Experimental data were then acquired in an uncooled rotating rig having the same upstream stator and four different rotor airfoil designs, including a conventional (baseline) configuration. Results from this three-phase program are discussed below followed by conclusions and recommendations for future work.

CFD CODE VALIDATION - (PHASE I)

Three dimensional Euler and RANS codes developed by Ni and Bogoian (Ref. 11) were used to conduct numerical experiments in the present work. The Euler code utilizes the explicit multiple-grid scheme presented by Ni (Ref. 12) on a structured three-dimensional mesh. The RANS code utilized is based on Ni's Euler solver. This code implements a second order accurate cell vertex scheme for the inviscid terms and a second order accurate method for the viscous terms. The viscous shear stresses are computed at the center of each control volume. A secondary control volume is then utilized to determine the rates of change of the shear stresses. The code employs a standard implementation of the Baldwin-Lomax (Ref. 13) turbulence model for wall bounded flows. Both Euler and RANS solvers are true multi-block codes which can compute the flow in multiple blade rows using non-reflective averaging plane inter-row boundary conditions. In addition, for rotors, flow in the tip clearance gap is solved using an embedded grid block which places the clearance mesh within the base rotor grid. In the present work, only isolated airfoil rows were modeled, therefore, the averaging plane boundary conditions were not employed.

Initial numerical computations were conducted by using the Euler code. A wall shear force model, similar to the one developed by Denton (Ref. 14), is used in this code to simulate the effects of blockage induced by viscous boundary layers. This code has been extensively used in the design of multistage turbines, and it has been shown to yield excellent estimates of airfoil loadings and spanwise distribution of gap averaged flow properties.

The flowfield was simulated in Sjolander's cascade (Ref. 3) with tip clearance using the RANS code. A total of 385,000 grid points were used through the airfoil passage and 28,000 points in the tip gap region. A schematic of grid topology is shown in Figure 5. Computed exit flowfield from this simulation is compared to the experimental data in Figure 6. The predicted flow structure in the tip region shows good agreement with the measured data. Additional simulations (not shown here) also were conducted for Moore's cascade (Ref. 5), and agreement between the predicted and measured results was found to be excellent, especially for the tip leakage induced flows. This exercise indicated that the 3D CFD codes could be used to provide fairly reliable estimates of flow features induced by tip leakage effects. RANS simulations were subsequently conducted for these same cascade configurations. The results from this calculation is similar results achieved by Liu and Bozzola (Ref. 15) and Mizuki and Tsujita (Ref. 16)

CONCEPT DEVELOPMENT - LINEAR CASCADES - (PHASE II)

Development of basic tip leakage flow/loss control concepts were executed for various airfoil configurations in linear cascades through the use of numerical and physical experiments. Cascades were chosen as the development vehicle because these allow cost effective assessment of the concepts at various levels of complexity.

Three cascades were designed for evaluation in a linear cascade facility. These cascades, termed as "baseline", "bowed", and "reverse bow", were built by using a single two-dimensional airfoil section in the spanwise direction. The airfoil sections for different configurations are tangentially offset to create a body force in the radial (spanwise) direction and to redistribute the flow. To assist in the understanding of tangential offset, assume an airfoil cross section is analogous to one card from a deck of cards, translate each card in the deck along one axis (tangential) and then smooth the steps between the cards (sections). With this concept of tangential off-set the "baseline" configuration forms an angle of 90 degrees between the suction side of the airfoil and the endwall (typical linear cascade), the suction surface of the "bowed" forms an angle of 130 degrees, and the suction surface of the reverse bow an angle of 65 degrees (these bowed airfoils are tangentially offset along a circular arc). For inviscid flow the base configuration will act 2-D across the span due to the absence of airfoil induced radial forces. With the tangentially offset airfoils there are radial components of flow induced by the three dimensional nature of the airfoils. The obtuse angle of the bowed airfoil's suction surface increases the static pressure at the wall and induces flow towards midspan, reducing the endwall loading and increases the loading at midspan. The reverse bow configuration induces flow towards the endwall increasing loading along the endwall and reducing the loading at midspan.

The effect of spanwise stacking of airfoil sections for these cascade configurations is shown in Figure 7. Airfoil surface static pressure distributions, calculated by using Ni's Euler

Code with a uniform inlet flow for the cascades with zero clearance, are shown in this figure at the midspan and the endwall. The bowed cascade shows reduced loading along the endwall relative to the base while the opposite is true for the reverse bowed cascade. If the tip leakage flow (vortex) is controlled by the pressure load in the endwall (tip) region, then this figure will indicate that the bowed airfoil is likely to generate a smaller tip leakage vortex than the baseline while the reverse bowed airfoil is expected to generate the largest tip leakage vortex out of these three cascades.

Flow simulations were conducted for the three cascades with two levels of clearances between the airfoils and the endwalls by using Ni's Euler and RANS codes. Figure 8 shows a comparison of the flowfield at the exit of the three cascades. It is clear from this figure that the bowed cascade yields the smallest tip clearance vortex while the reverse bowed cascade produces the largest vortex. The variation in the size of the vortices observed in this figure is in agreement with the hypothesis that the size of the tip leakage vortex is controlled by the pressure load in the endwall region. Further comments on the validity of this hypothesis are made in the later section of this paper.

Numerical data obtained from the above simulations were integrated in the spanwise and the tangential direction to determine an effective efficiency as it might appear in an actual turbine. Results from this processing are shown in Figure 9 where the baseline cascade is shown to have a sensitivity typically experienced with a rotor ($\Delta\eta \approx 2^*$ **clearance/span; i.e. k = 2**). The value of "k_{3D}" (equation 2) for the bowed and the reverse bowed airfoils are predicted to be 0.55 and 1.27, respectively. Results from this numerical study indicate that spanwise stacking of rotor airfoils can have a significant impact on the tip leakage vortex size and losses.

Physical experiments were conducted for the above three cascades to verify the numerical results. Three sets of airfoils were built for utilization in a linear cascade facility. A clearance to span of 5% was used for all three configurations. The flowfields were visually examined in a water flow tunnel (linear cascade facility) at the University of Connecticut. The flow visualization technique was a combination of electrolysis (to seed the flow), a laser (to view a plane), and a video camera (to record the results). To seed the flow, a length of wire is placed in the flow at the desired location, current is passed through the wire generating hydrogen bubbles, these bubbles convect downstream with the flow creating the seed (buoyancy of the bubbles were not significant). A laser plane was generated from the top of the tunnel and projected through the endwall at a 90 degree angle, with all but the laser light removed the hydrogen bubbles passing through the plane of light is clearly visible and can be recorded looking upstream from the rear of the tunnel.

Figure 10 shows a schematic of the cascade with several seed spans at the inlet and several laser planes through the cascade. A matrix of various inlet seeding and laser planes visualization was performed. The main result from these studies is that the tip leakage vortex structure is substantially affected by the three dimensional flow induced by spanwise stacking of the airfoils in the cascades. The size of the tip vortex is largest for the reverse bowed airfoil and smallest for the bowed airfoil which is in agreement with numerical simulations shown above (Figure 8).

Work conducted in this phase of the program clearly indicates that size of the tip leakage vortex can be substantially reduced by unloading the airfoil in the tip region through spanwise stacking (bowed airfoil). This design concept is supported by physical and numerical experiments conducted in a linear cascade configuration. Verification of this concept, in a rotating rig, is executed in the third phase of the program discussed in the remainder of this paper.

CONCEPT VERIFICATION - ROTATING RIG (PHASE - III)

Results presented above for the first two phases of the present program clearly show that: i) tip clearance vortex structures in linear cascades can be fairly well simulated by utilizing state-of-the-art 3D Euler or RANS codes (figure 6). ii) Size of the tip leakage vortices in linear cascades can be reduced by unloading the airfoils in the tip regions through appropriate stacking of airfoils in the spanwise direction (Figures 8 & 10).

If it is assumed that the size of the tip leakage vortex is a good indicator of the loss associated with the tip leakage flow, then the design concept to minimize the effect of tip leakage flow is fairly straightforward. The concept is to stack the rotor airfoil sections in such a manner that it reduces the static pressure difference on the two sides of the rotor airfoil in the tip region. This concept can be easily achieved by designing a bowed rotor airfoil. Three different designs of the bowed rotor airfoil were executed in the present program. Results from this design exercise are described below which are followed by details of the experimental program conducted to evaluate these designs and by discussion of the comparison between experimental data and theoretical results.

ROTOR AIRFOIL DESIGN AND STACKING

A conventionally designed single stage turbine was selected as the test article for the present investigation. Pertinent aerodynamic and geometric parameters for this turbine are given in Table 1. At the onset of the program it was decided that the same stator airfoil will be used with different rotors. In addition, it was decided that all rotor airfoils would maintain the same pertinent parameters (i.e. airfoil count, average loading, pitch/chord, aspect ratio, trailing edge thickness) The baseline rotor airfoil was redesigned to achieve reduced size of tip leakage vortices. Three different concepts for the rotor designs were used. A schematic of these rotor

airfoil geometries together with the baseline rotor are shown in Figure 11.

The baseline rotor was designed by using the "conventional" process of stacking 2-D airfoil sections radially in the spanwise direction. The first 3-D rotor airfoil, configuration-A, was designed by tangentially restacking the baseline airfoil sections consistent with the stacking conducted for the bowed linear cascade. The bowing of the rotor airfoil, however, is concentrated in the tip region similar to the bowed rotor design shown by Kingcombe et al. (Ref. 17). The second 3D rotor airfoil, configuration -B, incorporates a combination of backward sweep and tangential bow. A combination of bow and sweep produces greater radial body forces without increasing the bow. Airfoil cross sections for these two rotor designs are identical to the baseline sections. The third 3D rotor airfoil, configuration C, contains a combination of rotor airfoil section redesign, axial sweep, and tangential bow in the design. The intent of this design was to further reduce the loading in the tip region by redesigning the airfoil tip section with reverse curvature (pressure side) and increased thickness.

Static to total pressure ratios along the tip of rotor airfoils for the three 3-D designs are compared to those for the baseline rotor in Figure 12. Results plotted in this figure were obtained by utilizing Ni's Euler code for the four rotors operating with zero tip clearance downstream of the same stator. An analysis of the numerical data plotted in figure 12 indicates that the 3D airfoils have lower loadings (static pressure differences on the two sides of the rotor airfoil at the tip) and trailing edge diffusion values than the baseline rotor. The loadings (and trailing edge diffusion) for configurations A, B, and C are, respectively, 16% (4%), 18% (5%), and 34% (9%) lower relative to the baseline rotor. Results from this analysis indicate that, if the tip leakage loss is controlled by the magnitude of airfoil loadings and levels of trailing edge diffusion in the tip region, then configuration C will produce better performance relative to the other two 3D designs, and all 3-D rotors will demonstrate benefit over the baseline design.

Results from the above numerical simulations were also used to compute the flow in the tip regions of all of the rotors. The computed flow for configurations A, B, and C was found to be respectively 11%, 14%, and 19% relative to the baseline design. If the flow in the tip region is an indicator of the losses associated with tip flow, then configuration-C will yield best results, and configuration A will yield the worst results for the 3-D rotor designs.

Numerical simulations were also performed for the four rotor designs of a tip clearance to span ratio of 2.8% by using Ni's RANS code. Contour plots of total pressure at the exit of all four rotors are shown in Figure 14. This figure shows largest size of tip leakage vortex for the baseline rotor. For the 3-D rotors, configuration -A is predicted to have the largest vortex whereas configuration -C has the smallest vortex. If the size of the vortex structure is an indicator of performance, the results shown in Figure 14 indicate that configuration -C and A, respectively, will produce the largest and the smallest benefits for the 3-D rotor designs.

All of the above three 3-D rotors together with the baseline design were used in the experimental rig (discussed below) to establish relative performance of the rotor airfoils and to assess the impact of tip clearance change on the change in efficiency for each design.

Parameter	Value
Tt1	646 ^{0}F
Pt1/Pt2	2.02
Cx/U	0.38
H/U^2	1.344
Rep	0.37
No. Stator Vanes	32
No. Rotor Blades	39
Rtip - Blade (in.)	6.574
Cooling	0.0 %
Cl/h	1.4%, 2.8%
Meas. Accuracy	+/- 0.2% η

Table 1: Single stage turbine rig parameters.

EXPERIMENTAL DATA ACQUISITION

The rotor configurations were experimentally evaluated in a steady state turbine rig facility. The rig is a single stage turbine that contains inlet ducting and stator vane geometry consistent with small gas turbine engines, as shown in Figure 15. The aerodynamic design parameters, airfoil count, and accuracy of the measurements are summarized in Table 1. The uncooled efficiency (η) is based on the thermodynamic measurements (Pt,Tt) at the inlet and exit of the turbine using Equation 4.

$$\eta = \frac{1 - Tt2/Tt1}{1 - (Pt2/Pt1)^{(\gamma - 1)/\gamma}} \qquad [4]$$

The inlet stagnation pressure (Pt1) and temperature (Tt1) are measured in the upstream plenum (not shown). The exit stagnation pressure (Pt2) is located approximately four axial chords downstream of the rotor. The exit stagnation temperature is measured relatively far downstream in the exit plenum (not shown). This large downstream distance allows temperature mixing and reduces errors in the determination of efficiency (accuracy within +/- 0.2%). In addition to the measurement of stagnation pressure and temperature, the absolute frame gas angle was measured at the exit of the turbine stage at approximately 20% axial chord downstream of the rotor airfoil.

The tip clearance between the outer case and the rotor blade tip section was varied by utilizing annular rings specifically fabricated at a diameter consistent with the required running clearance. This method of clearance variation was preferred over grinding the rotor airfoil tips. Removal of material from 3-D rotor airfoils had the potential to alter the geometry and thus provide inaccurate assessment of the designs. Detailed experimental data were acquired by operating the rig over a range of pressure ratios and speeds. Data were acquired for two levels of tip clearance (clearance/span = 1.4% , 2.8%) for each rotor configuration.

DISCUSSION OF RESULTS

Experimental data acquired in the rotating rig at the design operating condition for the rotor is plotted in Figure 16. Data are given for all four rotor airfoils at the two levels of tip clearances tested. This figure shows change in efficiency as a function of the change of tip clearance between the lowest and the largest clearance levels ($\Delta\eta$ vs ΔCl). The resultant efficiency to tip clearance sensitivity (k_{3D}), is found to be 0.61, 0.7, and 0.86 for the configurations A, B, and C, respectively. This result clearly shows that all three 3-D rotors yielded lower loss in efficiency, due to a change in clearance, than that obtained for the baseline rotor. The relative change in the "k_{3D}" factor between the 3-D rotors are, however, not in agreement with pretest expectations (based on changes in airfoil loadings, trailing edge diffusion, and size of the predicted tip leakage vortices). All of these "features" indicated the lowest value of k_{3D} for configuration-C, followed by configuration-B, and -configuration-A.

The measured exit flow angles, in the absolute frame, are shown if Figure 17 for the four rotor configurations. Figure 17a shows that the exit gas angle for the conventional rotor, is influenced by tip clearance across the full span. In addition, this figure also exhibits the increase-decrease in gas angle in the outer portion of the span, which is typically associated with clearance. Figure 17b shows that the exit gas angle has the least spanwise penetration of all the rotor configurations. Figure 17b also exhibits the increase-decrease in angle in the outer portion of the span, but is reduced relative to the conventional design. Figures 17c and 17d both show that the influence of tip clearance penetrates down to approximately 20 percent of the span. The increase-decrease of the exit gas angle, in the outer portion of the span, is reduced relative to the other two configurations. These angle distributions suggests that the tip clearance vortex is reduced with the 3D rotors as predicted by the CFD analysis. In fact, the measured exit gas angle agrees with the expectation that the tip vortex size and strength would be reduced the least for configuration-A and the most for configuration-C, relative to the conventional design. In addition, the spanwise influence of tip clearance (penetration) on the spanwise exit gas angle approximately correlates with the sensitivity of efficiency with tip clearance.

In addition to the efficiency of the stage, the performance of any downstream airfoils must be considered in the optimization of a configuration. When the downstream airfoil operates in a flowfield with upstream distortions, the performance will be adversely affected. A comparison between the conventional design and configuration-A (the best performing configuration) shows that the 3D rotor produces less angle deviation than the conventional design (Figure 18). This figure shows that the change in rotor blade exit gas angle between two clearances (angle deviation) are reduced in the outer span region for configuration-A. This reduction of gas angle deviation not only indicates the benefit of the work extraction, it also indicates that an airfoil downstream of this stage will operate in a less distorted operating condition over operational clearances (indicative of typical hardware and speed variations).

CONCLUSION

- 3D rotor blade designs have been demonstrated to reduce the sensitivity of efficiency to tip clearance changes.
- The process of regulating spanwise flow distribution in the rotor blade (and/or reduced loading in the tip region) has shown to reduce efficiency sensitivity to clearance.
- Linear cascades can be used to study tip clearance concepts provided the information is properly utilized.
- Navier-Stokes and Euler codes can be used to guide the design of geometry to desensitize the efficiency to tip clearance.

NOMENCLATURE

C Velocity
U Tangential Wheel Speed
H Turbine Work
η Turbine Efficiency
Cl Tip Clearance
h Span
P Pressure
T Temperature
Rep Pressure Reaction
R Radius
B Chord
N RPM
γ Specific Heat Ratio
k Constant of proportionality

Prefix:
Δ Change of a Parameter (i.e. $\Delta\eta$)

Subscript:
x Axial Direction
t Stagnation Conditions
s Static Conditions

1 Rig Inlet
2 Rig Exit
tip Tip of the Rotor Blade

ACKNOWLEDGMENTS

The authors wish to thank Pratt and Whitney for permission to publish this work, Dr. S. Kacker for providing rig facilities at Pratt and Whitney Canada, Dr. R. Ni for CFD support, R. Lee for early design concepts, Dr. L. Langston for providing the water tunnel facilities at University of Connecticut, and finally Shankar Magge and Gary Paron for design support.

REFERENCES

1) Booth, T.C., "Importance of Tip Clearance Flows in Turbine Design", VKI Lecture Series 1985-05.

2) Yamamoto, A., "Endwall Flow / Loss Mechanisms in a Linear Turbine Cascade with Blade Tip Clearance", ASME Paper No. 88-GT-235.

3.) Sjolander, S.A., Amrud, K.K., Effects of Tip Clearance on Blade Loading in a Planar Cascade of Turbine Blades", J. OF TURBOMACHINERY, Vol. 109, pp. 237 - 245.

4.) Yaras, M., Yingkang, Z., Sjolander, S.A., "Flow Field in Tip Gap of a Planar Cascade of Turbine Blades", Presented at the Gas Turbine and Aeroengine Congress and Exposition, June 5-9, 1988, Amsterdam, Netherlands.

5.) Moore, J., and Tilton, J.S., "Tip Leakage Flow in a Linear Turbine Cascade", JOURNAL OF TURBOMACHINERY, Vol. 110, pp. 301-309, 1988.

6.) Bindon, J.P., "The Measurement and Formation of Tip Clearance Loss", ASME Paper No. 88-GT-203.

7.) Lakshminarayana, B., 1970, "Method for Predicting the Tip Clearance Effects in Axial Flow Turbomachinery," ASME J. OF BASIC ENG., Vol. 92, pp. 467-481.

8.) Lakshminarayana, B., Horlock, J.H., 1965, "Leakage and Secondary Flows in Compressor Cascades," ARC R&M No. 3483.

9.) Chen, G. T., Greitzer, E.M., Tan, C.S., and Marble, F.E., "Similarity Analysis of Compressor Tip Clearance Flow Structure," ASME J. OF TURBOMACHINERY, Vol. 113, pp. 260-271.

10.) Dietrichs, H. -J., Malzacher, F., Broichhausen, K.,"DEVELOPMENT OF A HP-TURBINE FOR A SMALL HELICOPTER ENGINE" , AGARD Presentation, Montreal, 1993 pp. 27.1 - 27.8.

11.) Ni., R., Bogoian, J.C., "Prediction of 3D Multi-Stage Turbine Flow Field Using a Multi-Grid Euler Solver", AIAA Paper 89-02032

12.) Ni, R., "A Multiple Grid Scheme for Solving the Euler Equations", AIAA Paper 81-1025R

13.) Baldwin, B., and Lomax, H., "Thin Layer Approximation and Algebraic Model for Separated Turbulent Flows," AIAA 78-0257, 1978.

14.) Denton, J.D., "The use of a Distributed Body Force to Simulate Viscous Flow in 3D Flow Calculations," ASME Paper 86-GT-144.

15.) Liu, J.S. and Bozzola, R., "Three-Dimensional Navier-Stokes Analysis of the Tip Clearance Flow in Linear Cascades," AIAA Paper 93-0391, 1993.

16.) Mizuki, S. and Tsujita, H., "Numerical Calculation of Flow For Cascade With Tip Clearance," ASME Paper 94-GT-361, 1994.

17.) Kingcombe, R.C., Bryce, J.D., Steeden, R.V., "The design and test of turbine rotor blade for reduced overtip loss", Institute of Mechanical Engineers Conference; Titled: "European Conference on Turbomachinery", Book Title; "Turbomachinery: Latest Developments in a Changing Scene", V. No. 1991-1993, Report No. CONF-9103254, C423/013, pp. 293-301, 1991.

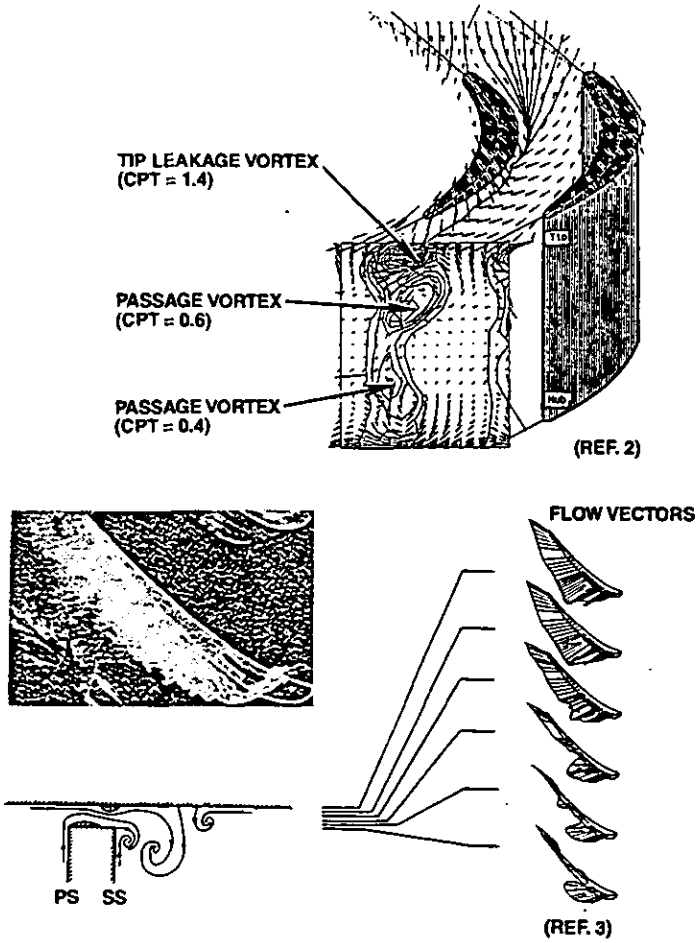

Figure 1 Tip leakage flowfield is a complex system of multiple separations, reattachments, and vortices (Yamamto-Ref. 2, Sjolander-Ref. 3). (CPT = {Ptexit - Ptinlet-midspan} / {0.5pV² inlet-midspan})

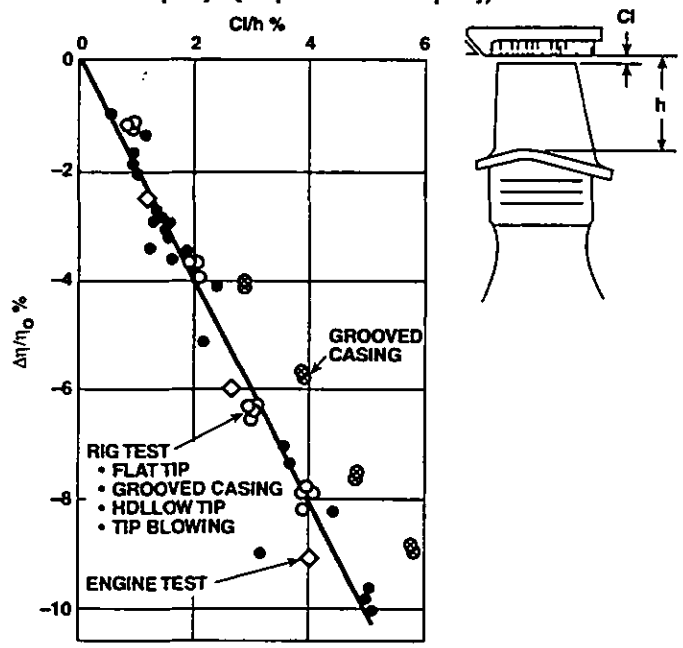

Figure 2 Historical data shows that the change in efficiency is proportional to the normalized tip clearance (Dietrichs et al.- Ref. 10).

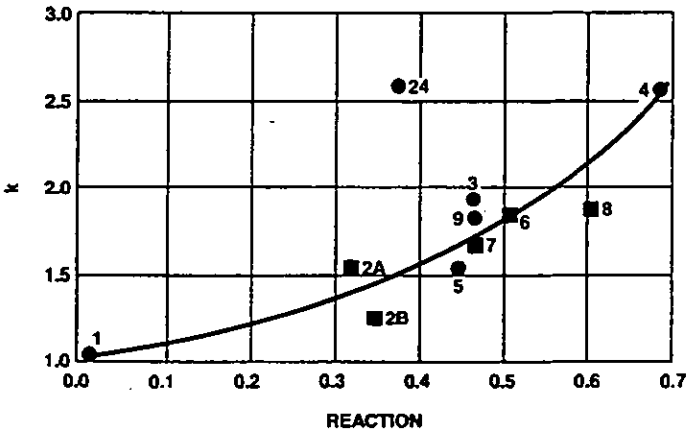

Figure 3 The constant of proportionality (k) is a function of reaction (Booth - Ref. 10).

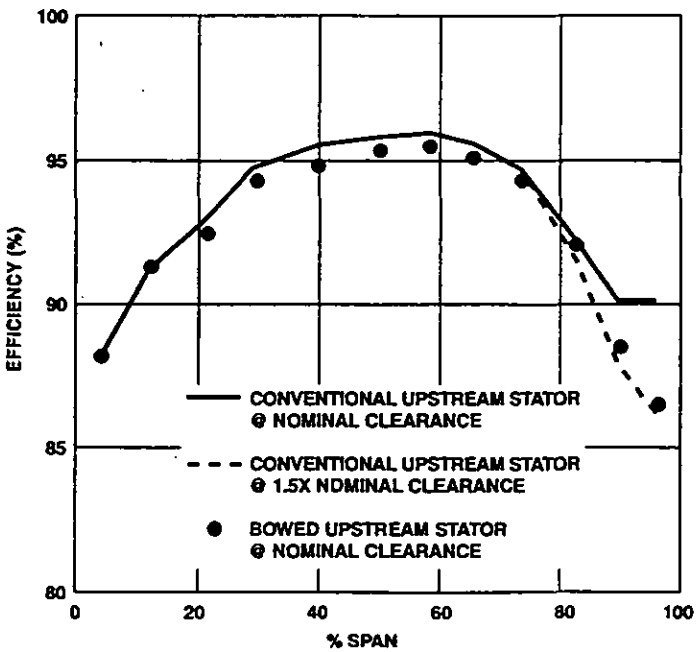

Figure 4 Turbine efficiency, in the tip region of a rotor, is affected by the upstream stator.

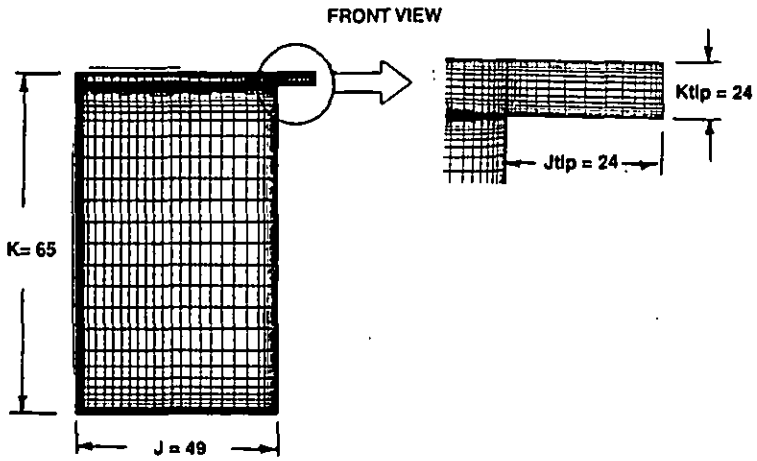

Figure 5 RANS computational mesh used to resolve the tip leakage flow for Sjolander's cascade (Ref. 3).

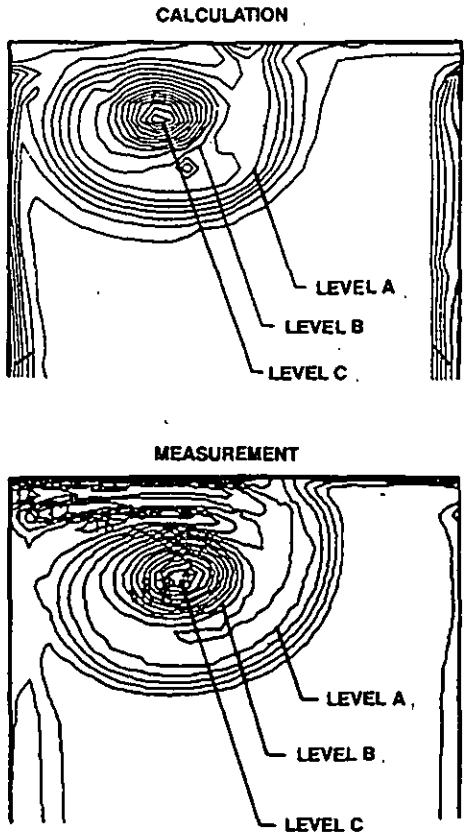

Figure 6 Total pressure coefficient contours at the trailing edge plane of Sjolander's cascade (Ref. 3) show good agreement between numerical simulations and data.

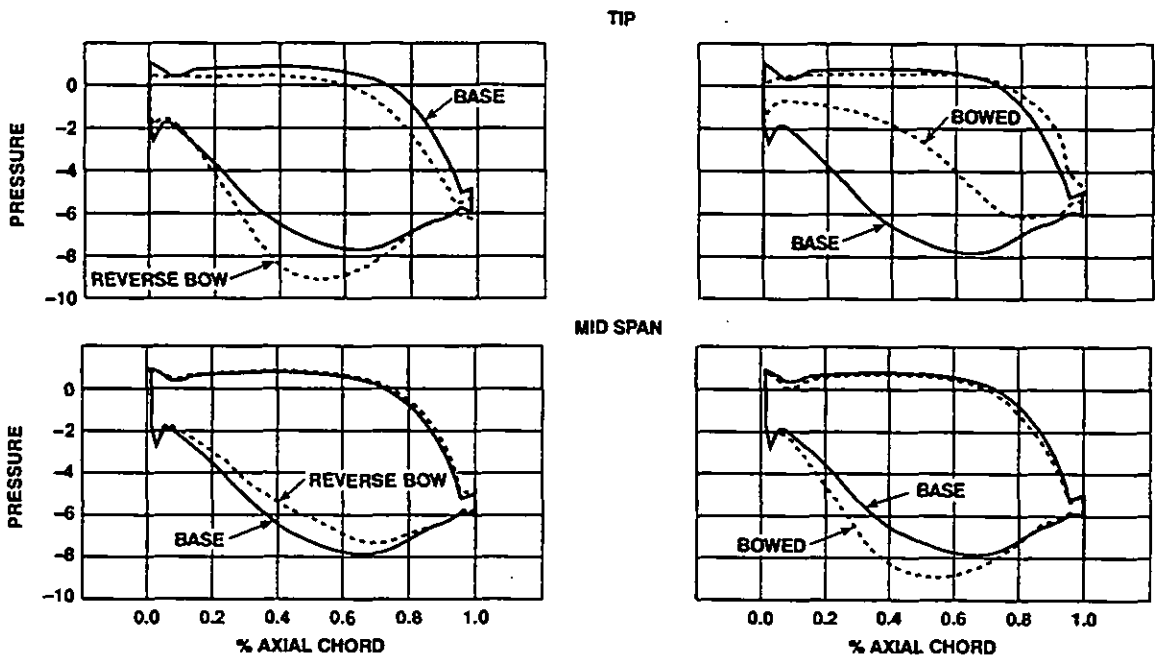

Figure 7 The bowed cascade design redistributes pressure loading away from the tip region towards the mid span, resulting in a lower "driving" pressure across the tip gap.

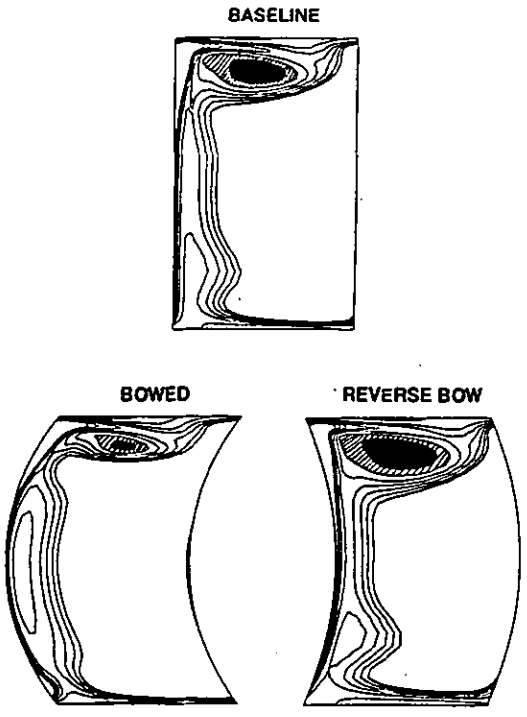

Figure 8 RANS simulations of the 3-dimensional cascade designs show the bow reduces the tip leakage vortex size. Loss contours at the airfoil exit plan.

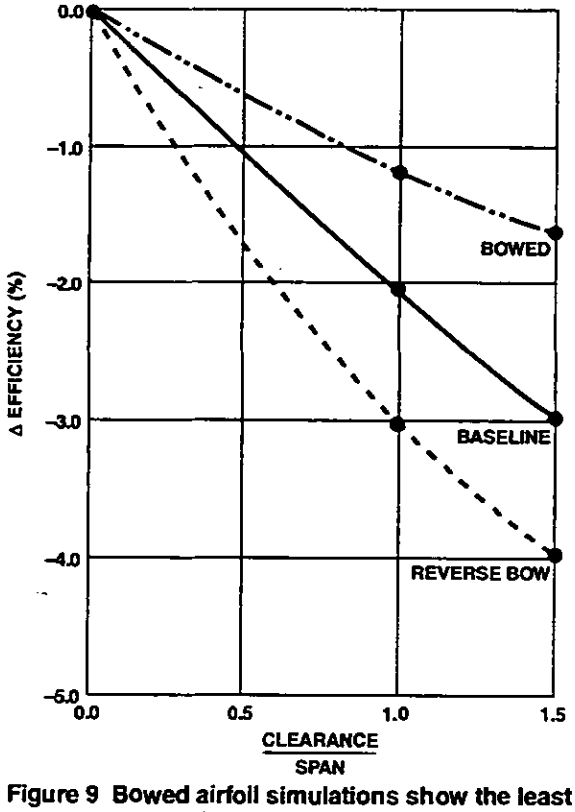

Figure 9 Bowed airfoil simulations show the least sensitivity to tip clearance relative to the baseline and reverse bow geometry for the linerar cascade.

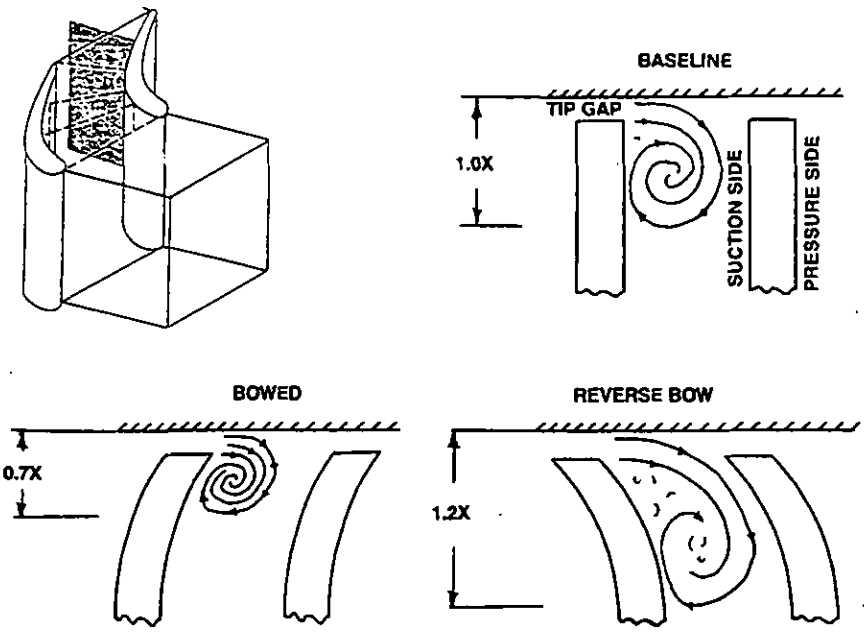

Figure 10 Flow visualization performed in a water tunnel show that the tip vortex is reduced in size when the airfoil is bowed.

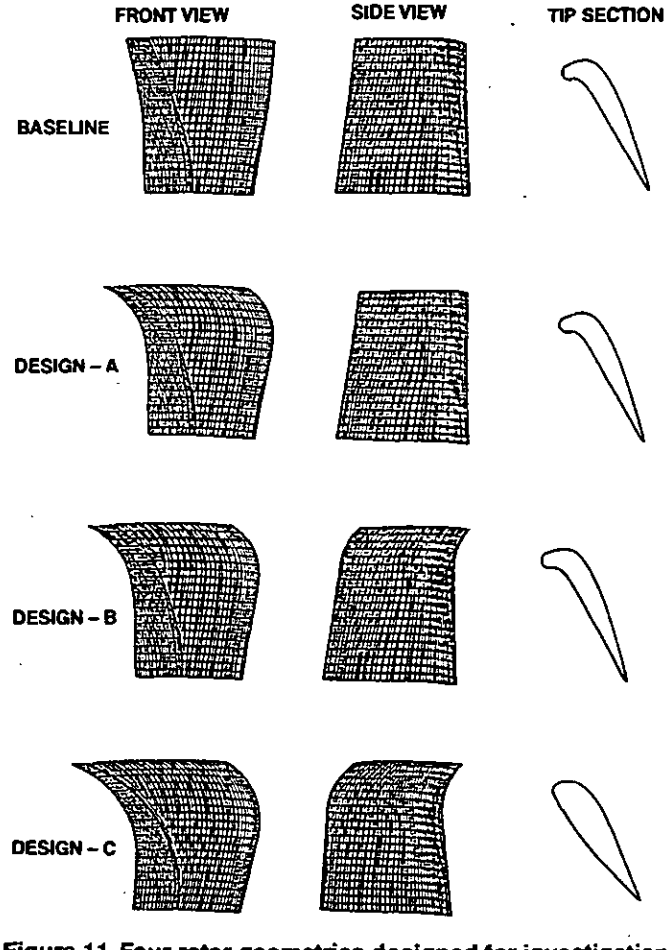

Figure 11 Four rotor geometries designed for investigation in a rotating rig: baseline, configuration-A (bowed), configuration-B (bow + sweep), configuration-C (bow + sweep + increased tip thickness).

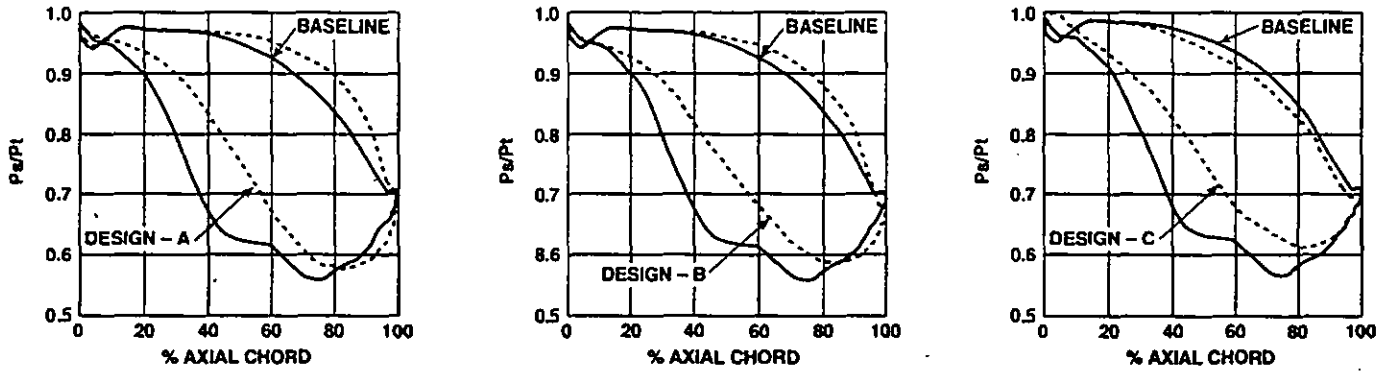

Figure 12 Three dimensional rotor airfoils show reduced loading at the tip.

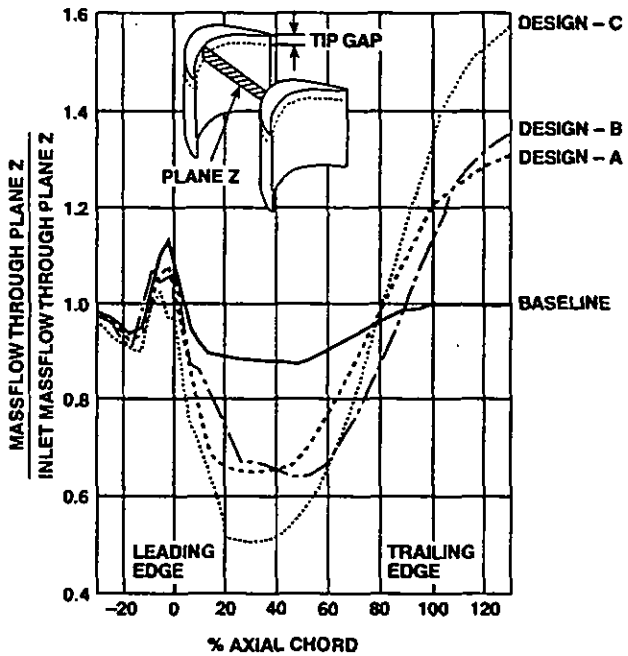

Figure 13 Three dimensional rotors yield reduced mass flow in the tip clearance portion of the Annulus as depicted by plane Z.

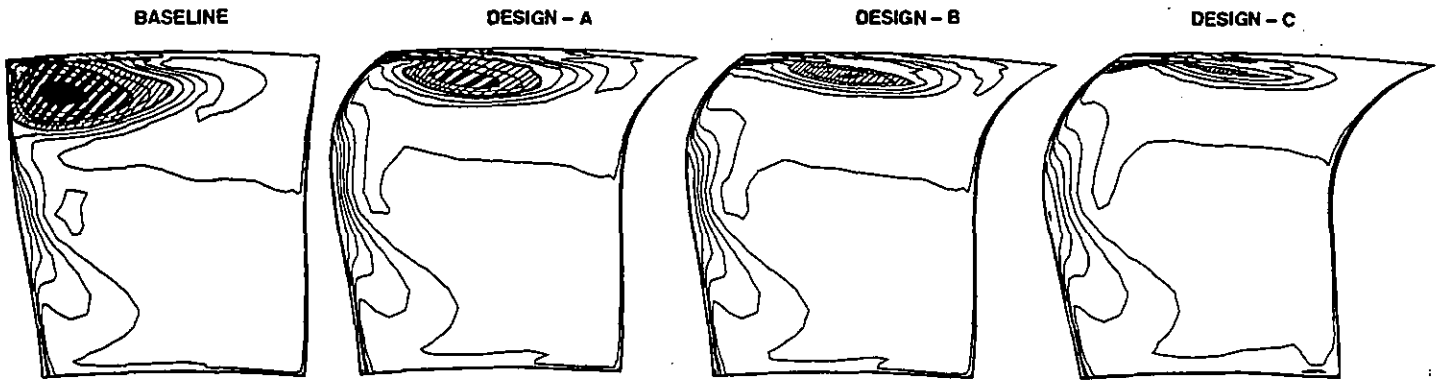

Figure 14 Three dimensional rotors designed to reduce the size of the tip leakage vortex.

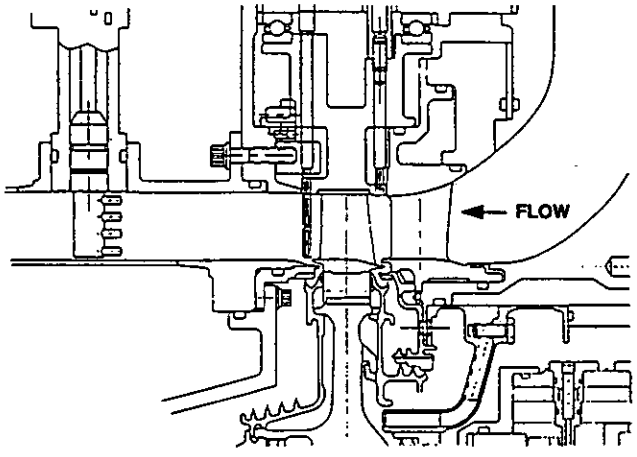

Figure 15 Elevation of the full scale uncooled single stage rotating rig configuration.

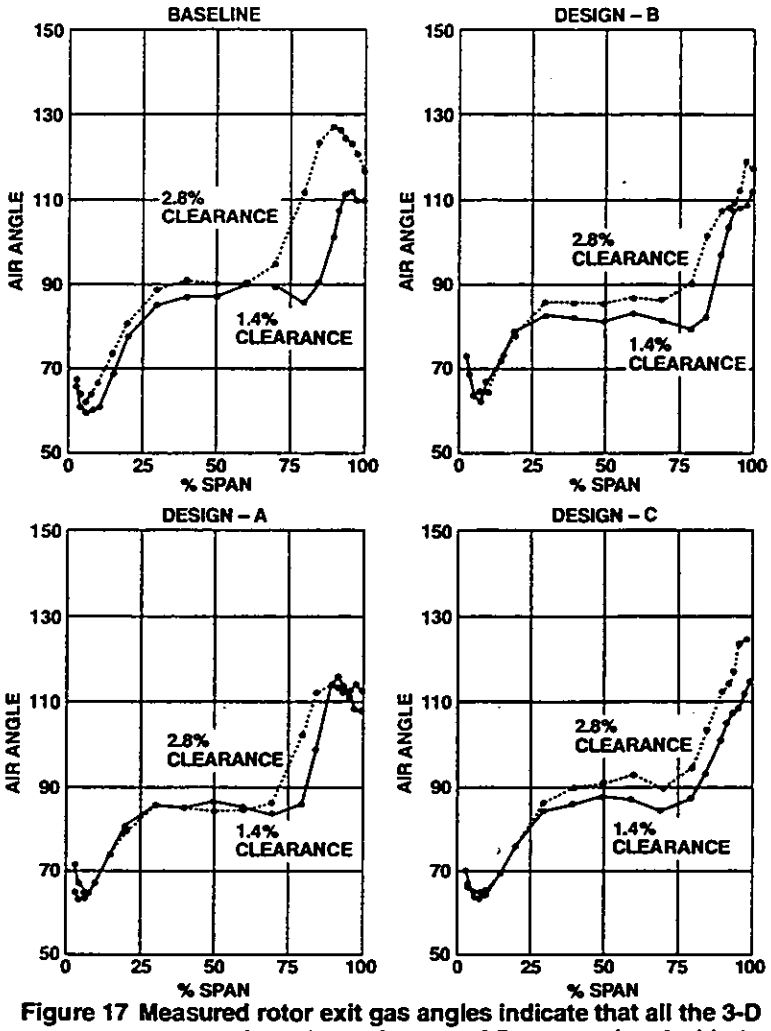

Figure 17 Measured rotor exit gas angles indicate that all the 3-D rotors reduce the under turned flow associated with the tip clearance vortex.

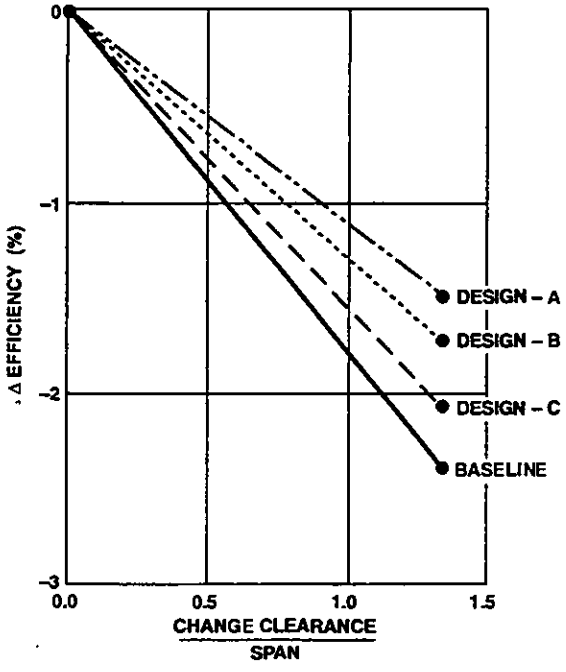

Figure 16 Experimental data show that all 3-D rotors reduce the sensitivity to tip clearance.

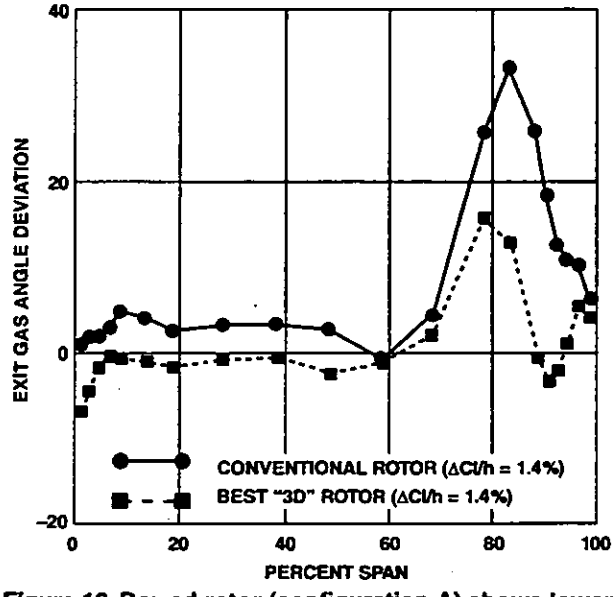

Figure 18 Bowed rotor (configuration-A) shows lower deviation of exit air angle due to the effect of clearance change than the baseline design.